# Performance of Ventilation Filtration Technologies on Characteristic Traffic Related Aerosol Down to Nanocluster Size

**Panu Karjalainen[1], Sampo Saari[1], Heino Kuuluvainen[1], Tapio Kalliohaka[2], Aimo Taipale[2] and Topi Rönkkö[1]**

*[1]Aerosol Physics Laboratory, Department of Physics, Tampere University of Technology, P.O.Box 692, FI-33101, Tampere, Finland*

*[2]Clean air solutions, VTT Technical Research Centre of Finland Ltd., Tampere, Finland*

## Abstract

Near traffic routes and urban areas, the outdoor air particle number concentration is typically dominated by ultrafine particles. These particles can enter into the nearby buildings affecting the human exposure on ultrafine particles indoors. In this study, we demonstrate an aerosol generation system which mimics the characteristic traffic related aerosol. The aerosol generation system was used to determine the size-resolved particle filtration efficiencies of five typical commercial filters in the particle diameter range of 1.3–120 nm. Two different HEPA filters were observed to be efficient in all particle sizes. A fibrous filter (F7) was efficient at small particle sizes representing the nucleation mode of traffic related aerosol, but its efficiency decreased down to 60% with the increasing particle size. In contrast, the filtration efficiency of an electrostatic precipitator (ESP) increased as a function of the particle size, being more efficient for the soot mode of traffic related aerosol than for the nucleation mode. An electret filter with a

charger was relatively efficient (filtration efficiency > 85%) at all the observed particle sizes. The HEPA, F7 and electret filters were found to practically remove the particles/nanoclusters smaller than 3 nm. All in all, the filtration efficiencies were observed to be strongly dependent on the particle size and significant differences were found between different filters. Based on these results, we suggest that the particulate filter test standards should be extended to cover the ultrafine particles, which dominate the particle concentrations in outdoor air and are hazardous for public health.

***Keywords:*** aerosol generation, traffic aerosol, filtration efficiency, particulate filter, ultrafine particles, filtration

## INTRODUCTION

Inhalable fine particulate matter, PM2.5 (mass of particles below 2.5 µm in diameter) has been observed to be a hazardous air pollutant in outdoor environments (Pope III, 1995; Lelieveld et al., 2015) and in indoor environments (Hänninen et al., 2011). Also ultrafine particles (UFP, defined as having a diameter of 0.1 µm or less) have been suggested to pose health risks due to their ability to reach the alveolar area of lungs (Wichmann and Peters, 2000; Oberdörster et al., 2001; Oberdörster et al., 2005; Li et al., 2003). Often majority of the vehicle exhaust particle number belongs to the UFP. On the other hand, World Health Organization (2012) reported that there was sufficient evidence of the carcinogenicity of diesel engine exhaust for humans. In general, large human populations are exposed to traffic related particles in everyday life.

In several studies, the urban air particle number size distribution measurements have shown that near traffic routes and in city centres the particle number is dominated by the UFP (Kittelson et al., 2004; Wehner et al., 2002; Ketzel et al., 2003; Longley et al., 2003; Virtanen et al., 2006; Pirjola et al., 2012; Lähde et al., 2014). In these cases, the mean particle size in urban air has been observed to be even smaller than 30 nm. Especially in traffic environments the UFP are emitted to the urban air mainly from traffic, by both gasoline (see e.g. Karjalainen et al., 2014) and diesel vehicles (e.g. Rönkkö et al., 2006). In addition to nanoparticles containing mainly semi-volatile sulphur compounds and organics (Tobias et al., 2001; Schneider et al., 2005; Rönkkö et al., 2007), diesel and gasoline vehicles can emit metallic nanoparticles (Rönkkö et al., 2014; Karjalainen et al., 2014) and soot particles (Heywood, 1989; Harris and Maricq, 2001), both contributing also on the UFP size range. In the vehicle exhaust particle number size distribution, particles with different structure and chemical composition are typically seen in different modes, which are a nucleation mode (NM) and a soot mode (SM). These traffic-related modes have been observed also in urban air quality studies near traffic routes. In addition to these modes, the urban aerosol is also affected by other sources and atmospheric aging. However, the traffic-related modes have been shown to dominate the lung deposited surface area (LDSA) size distributions in urban environments (Kuuluvainen et al., 2016). The LDSA is a metric for the potential negative health effects of aerosol particles.

In polluted areas, the outdoor particle concentration can affect significantly the indoor air particle concentrations in buildings (Quang et al., 2013; Morawska et al., 2013; Hussein et al., 2005; Hussein et al., 2015). Due to that, especially in the buildings near heavy traffic areas, indoor air may contain significant amounts of vehicle exhaust originated UFP. Particle filtration in ventilation systems can be seen as a key technology to prevent health risks of these particles (Nazaroff et al., 2004). According to the classical filtration theory, the mechanical fibrous filters

are relatively effective for removing very small particles due to the diffusion mechanism (Friedlander, 1958, Hinds 1982). Shi et al. (2013) reported that the filtration efficiency of UFP varied between different intermediate bag filters, designed for general ventilation applications, and was influenced, for instance, by the air velocity and the electrical properties of the filter media. However, it is not very well known how the building ventilation and filtration systems or the room air cleaners affect the UFP concentrations. Especially, the number of studies focusing on the size dependency of filtration efficiencies in the UFP size range is limited.

The optical particle measurement technologies utilized in filter standards, such as EN779-2012, ASTM F1471-2009, EN 1822-2009 and ASHRAE 52.2-2012, cannot detect particles in the UFP size range, which means that the filtration efficiency for the UFP is not measured in the standard tests. The standard test particle generators producing DEHS particles (EN779-2012) or KCl particles (ASHRAE 52.2-2012) are not typically used in the UFP size range, although these methods can be used to generate particles in the ultrafine particle size range. An exception is the HEPA test standard (ISO 29463), where DEHS is one of the test materials, for which the particle size range is down to 0.04 micron. Loading aerosols used in laboratory measurements (ISO Fine and ASHRAE test dust) mainly consist of particles above 1000 nm, and therefore the standard tests are not able to predict properly the filter performance under real operation conditions. While the DEHS and KCl particles are typically used in filter testing, few studies for the filter loading characteristics have been also with real soot particles (e.g. Kim et al., 2009; Valmari et al., 2006; Chen et al., 2017).

In this study, we demonstrate a test aerosol generation system which mimics the characteristics of engine exhaust aerosol dominating the particle number concentration in urban environments. The test aerosol generation system produces not only the typical particle size distribution but also the physical and chemical characteristics of particles. In addition, the generation system is used in

this study to determine the ultrafine particle filtration efficiencies down to 1.3 nm in particle size of typical commercial filtration solutions, including a fibrous filter, HEPA filter, electrostatic fibrous filter and an electrostatic precipitator.

# METHODS

### *Test aerosol generation system*

The test aerosol generation system consists of a nucleation mode (NM) particle generator and soot mode (SM) particle generator (Fig. 1). The NM generator aims to reproduce the sulphur driven nucleation particle formation process (Arnold et al., 2012) by a controllable way. In the generator, $SO_2$ gas is oxidized to $SO_3$ at high temperature in a catalytic converter (see e.g. Giechaskiel et al., 2007; Karjalainen et al., 2014b). Oxidized $SO_3$ then reacts with water molecules forming gaseous sulphur acid (GSA) (Arnold et al., 2012). This high temperature gas is further mixed with cool air, which leads to the formation of nucleation mode particles. The size of these particles is typically in the range of 3-30 nm. The SM generator is a common small sized boat diesel engine (Yanmar L40E-D operated at 750 W power). The initial NM formation occurs upstream of the SM generator inlet in order to minimize condensation losses to existing soot particles. In our system, the NM particles and SM particles are mixed, and the resulted aerosol is stabilized in the mixing chamber with the volume of ~5 $m^3$. The particle generation system enables the filter tests with typical flow rates of ventilation filters.

### *Test filters*

The particle generation system was applied to study the filtration efficiency of five different commercial particle filters. The first filter was a mechanical bag-type glass fiber filter graded to the class F7 according to EN779. The second and third test filters were high-efficiency particulate arrestance (HEPA) filters, called HEPA 1 (graded to the class H12) and HEPA 2 (graded to the

class 13) here. The fourth test filter was an electret filter including a wire-type particle charger and an electrostatic filter media. The electret filter was studied both with (w/) and without (w/o) the charger. The fifth test filter was a two-stage electrostatic precipitator (ESP), including a wire-type particle charger region and a collection stage made of aluminum plates. The charger and collection voltages in the ESP were 7.5 kV and 4.0 kV, respectively, and the corona current was 1 mA. Schematic figures and details of the test filters are shown in Table 1.

The tested filters were fixed tightly in the duct downstream of the mixing chamber and the air flow through the filter was fixed to the desired value. In these tests, the face velocity was varying according to designed application resulting flow rates between 50 l/s and 500 l/s through the filters 1-5. With these flow rates, pressure drops over the filters varied between 3 Pa and 152 Pa, respectively. Since both the particle generators are thermal systems that require stabilized temperatures, the generators were turned on at least one hour before the actual efficiency measurements to ensure a constant concentration and a stable particle size distribution during the measurement.

***Sampling and measurements***

The test aerosol sample was taken from the ventilation channel via two sampling probes, one upstream and the other downstream of the test filter (see Figure 1). An automated valve was used to switch the sampling lines at a 12-minute interval. The sequential upstream and downstream measurement cycle was repeated three times for every test filter. After sampling, the aerosol was diluted by an ejector type diluter (Dekati Diluter, dilution ratio of c. 8) and then conducted to measurement instruments. The filtration efficiencies were studied in a wide particle size range, but especially with ultrafine particles down to 1.3 nm. A particle size magnifier (PSM, Airmodus A10) (Vanhanen et al. 2010) and two scanning mobility particle sizers (Nano-SMPS and Long-

SMPS, TSI Inc.) were used to measure particle number size distribution in the size ranges of 1.3-2.9 nm (PSM), 3-65 nm (Nano-SMPS) and 10-450 nm (Long-SMPS). A small-scale ESP (Mini-ESP, similar as used e.g. in Karjalainen et al. (2014b)) was applied to study the subsets of charged and uncharged particles. The Mini-ESP was installed upstream of the Long-SMPS, and it operated with the flow of 0.6 lpm. Using a voltage of 3 kV in the Mini-ESP, based on the experimental data, charged particles below 100 nm in diameter were removed. An electrical low pressure impactor (ELPI, manufactured by Dekati Oy) (Keskinen et al., 1992) was used to monitor the particle concentration with a high time resolution. A $CO_2$ analyzer (SICK Maihak, Sidor) was used in the setup in order to monitor that the dilution ratio in the ejector diluter was constant, so that it did not change when the aerosol flow was changed between the upstream and downstream sampling. Simultaneously, the stability of $CO_2$ concentration was used to monitor the stability of the SM generator.

## RESULTS AND DISCUSSION

### *Test aerosol*

Fig. 2 shows a typical particle size distribution of the generated aerosol measured from the upstream of the test filter after the dilution (dilution ratio ~8). The mean particle sizes (mean particle diameters) of the nucleation mode (NM) and soot mode (SM) were 11 nm and 55 nm, respectively. There were measurable but small particle concentrations of NM particles also in the PSM particle size range (inside panel in Figure 3). The relative concentrations in the modes were adjusted by controlling the exhaust flow of the SM generator. When compared, e.g. to the typical real-world fresh diesel exhaust aerosol (Rönkkö et al., 2006; Karjalainen et al., 2014b), it can be seen that the generation system reproduced the exhaust particle size distribution and the relative concentrations of the two particle modes well.

It should be noted that also the characteristics of particles were, at least qualitatively, similar than in real exhaust; generated nanoparticles were semivolatile and consisted of sulphur compounds whereas the larger particles were mainly solid soot particles. Based on the size distribution data and the usage of the Mini-ESP, the particles smaller than 50 nm were electrically neutral, but the larger soot particles were partially charged so that over a half of the particles at 100 nm was electrically charged. Therefore, basically the whole NM was uncharged, similarly as in Karjalainen et al. (2014b), but large soot particles were partially charged (Maricq et al., 2006). The effects of the original charging state of particles on the filtration efficiency are discussed below.

Fig. 3, the upper pane, shows the time series of the particle number concentrations for the nucleation and soot modes calculated from the size distributions upstream and downstream of the tested filters (Nano-SMPS, $D_p$ < 20 nm, for nucleation mode and Long-SMPS, $D_p$ > 20 nm, for soot mode). The lower pane of Fig. 3 shows the total particle concentrations measured by the ELPI. For all instruments, the higher concentrations were measured upstream of the test filter, while the lower concentrations were measured downstream. When sampled upstream of the filter, the NM number concentrations were 4–10 times the SM concentrations. This is also seen from the ELPI data which only measured particles larger than 30 nm. For F7 and HEPA 1 filters, the NM concentration was higher compared to other filter tests because of different flow rates and

dilution ratios used in the generator part. The particle concentration remained relatively stable through each test. However, there were decreasing trends in the soot mode concentrations in the cases of F7 and the electret filter with a charger. However, the variation in the particle concentration was not significant in larger time scales. The sampling was periodically performed both upstream and downstream of the filter to avoid systematic error, and hence the particle filtration tests produced reliable and comparable results.

***Filtration efficiency***

Differences in filtration efficiency between the tested filters were observed to be significant (see Fig. 4). Almost all the particles smaller than 3 nm in diameter were removed in all the filters. This is explained by the rapid diffusion motion of these nanoparticles and thus the particle losses in the filters were remarkably high regardless of the different filtration techniques. However, for the particles larger than 3 nm, the general trends of the filtration efficiency as a function of the particle size showed significant differences between the different filtration techniques. In general the relative error increased towards the lower and upper detectable particle sizes (shown in Fig. S1) but the error levels were in general low. Most relative error values were below 5 %-points even though especially for the ESP values were greater below 5 nm and above 150 nm. There was also an increased relative error in the particle size area between NM and SM (~20 nm). The relative error (as percentage points) was naturally dependent on the filtration efficiency values, so that e.g. for HEPA 1 the values were below 0.1%-points below 100 nm particle sizes.

In the case of F7, the collection efficiency was practically 100% up to the particle diameter of 10 nm and decreased steeply in the particle size range above 20 nm. Hence, the F7 was efficient filter for the NM particles but less efficient for the SM particles. The particle filtration efficiency of F7 type filters is typically dominated by the diffusion, impaction and interception processes of the particles in the filter media (Friedlander, 1958; Shi et al., 2012). The F7 filtration efficiency curve observed in Fig. 4 was in line with the previous studies (e.g. Shi et al., 2012; Goodfellow et al., 2001) having the most penetrating particle size (MPPS) roughly at 200 nm wherein filtration efficiency was around 50%. The diffusion motion of particles increases in smaller particle sizes, and therefore the observed filtration efficiency was high for the particles below 20 nm. Kim et al. (2006, 2007) reported also that the particle penetration in glass fiber filters decreases continuously down to 3 nm as expected from the classical filtration theory. They suggest that the

thermal rebound phenomena would be operative for nanoparticles with diameters below 2 nm, even though it would depend on the states of both the particles and the filter media (Kim et al., 2006). In this study, we did not find the thermal rebound of NM particles although our measurement range covered particle diameters down to 1.3 nm.

Compared to the F7 filter, the ESP was not that efficient at small particle sizes but the particle filtration efficiency increased as a function of particle size; in particle sizes 4–10 nm the collection efficiency was lower than 50%, at 20 nm it was 70% and at 40 nm it reached a level of 95%, so the ESP was efficient for the SM particles but less efficient for the NM particles. It should be noted that, for the ESP, a collection efficiency of 100% was not observed at any particle sizes. This is probably due to the charging efficiency of the ESP charger (part of the particles remains electrically neutral in all particle sizes). The functioning of the ESP is based on the electrical charging of particles using a corona charger and collecting the charged particles using an electric field (Jaworek et al., 2007). The collection efficiency of ESP depends on the charging efficiency, number of elemental charges and electrical mobility of particles as well as the geometry of the device. The charging efficiency of corona chargers typically decreases in smaller particle sizes (Kulkarni et al., 2011), and thus the filtration efficiency was low for particles below 30 nm in this study. The low filtration efficiency of the ESP devices for small nanoparticles was also reported by Huang et al. (2002). They stated that aerosol penetration through the single- and two-stage ESPs increased significantly for particles below 20 and 50 nm, respectively. The observation that the filtration efficiency again increased when the particle size decreased below 3 nm is likely due to the diffusional filtration mechanisms of neutral particles, not because of electrical filtration since particle charging probability is likely very small. Note however that there was a high relative error in the determination of filtration efficiency for the ESP in particle sizes below c. 6 nm.

The electret filter represents a modern filter type including both a wire-type particle charger and an electrostatic filter media. The filtration efficiency of the electret filter with a charger was above 90% for both the NM and the SM in the size range of 4.5–200 nm (see Fig. 4). Both the ESP and F7 filter characteristics are combined in the electret resulting in high particle removal performance in a wide size range with relatively low pressure drop. The filtration efficiency without a charger represents the performance of the electrostatic filter alone. In this case, particles below 20 nm are removed by diffusion similarly as in the F7 but with lower performance. The

filtration efficiency decreased for the particles larger than 20 nm but increased again for the particles larger than 50 nm. This can be explained by increasing fraction of the originally charged SM particles in the size range above 50 nm, as shown in Fig. 2. Electrostatic filter media have typically higher filtration efficiency for charged particles compared to neutral particles (Shi 2012, Romay et al., 1998).

The filtration efficiencies of both HEPA filters were above 99% in the test particle size range. The HEPA 1 collected 99.99% of NM particles and 99.95% of SM particles, whereas the filtration efficiencies of the HEPA 2 were 99.60% and 99.33% for the NM and the SM particles, respectively. The results showed that both the HEPA filters worked very well, even though the penetrated particle number for the HEPA 1 was over 10 times less than for the HEPA 2.

The most penetrating particle size (MPPS) was calculated for the test filters based on the filtration efficiency curves (Fig. 4). For each filter, the filtration efficiency was converted to the penetration and a quadratic function was fitted to the data at the neighborhood of the local maximum of the penetration. The obtained MPPS values were >200 nm, 34 nm, 32 nm, 20 nm, 50 nm and 6.2 nm for the F7, HEPA1, HEPA2, Electret w/ charger, Electret w/o charger and ESP, respectively. With the exception of F7, all the test filters had the MPPS in the ultrafine particle size range. The MPPS results are reasonable if compared to previous studies. Chang et al. (2015) reported MPPS values between 10 and 30 nm for pleated HVAC electret filters at face velocities between 0.05 and 1 m/s. A previous study by Sinclair (1976) showed that the typical MPPS value for a HEPA filter was about 40 nm at a flow rate of 70 cm/s. Alderman et al. (2008) reported the MPPS values of 110–130 nm for HEPA filters at low face velocities (2.0–4.5 cm/s). The MPPS values typically increase with lower face velocities (Lee and Liu, 1980). Chen et al. (2017) reported that MPPS values were about 200 nm for two fiber filter types, however the MPPS values were sensitive of filter loading so that with increased loading the size decreased by 20-50 nm depending on the filter type. It should be noticed that most of the filters tested in this study had the MPPS at the same particle size range as the dominant outdoor aerosol.

While the particle size resolved filtration efficiencies are highly beneficial in the evaluation of filtration technologies, the final effectiveness of the technologies can be evaluated only if the aerosol, especially the aerosol particle size distribution, is known. In urban areas the particle size distribution varies significantly; while the smallest particle sizes are typically measured near

traffic, the mean particle size of urban background aerosol is often larger. Fig. 5 simulates the effectiveness of the filter types studied above for different urban aerosols, simultaneously aiming to show how the studied filter technologies can affect indoor air particles in different environments. Fig. 5 includes both total filtration efficiencies (TFE) for particles and the size distributions of particles penetrated the studied filters. The TFE and size distributions were calculated for test aerosols used in this study (nucleation mode, soot mode, both modes), and then with real ambient aerosols measured next to a major road in Helsinki (Helsinki, road side, Virtanen et al., 2006), at an urban background station in Beijing (Beijing summer, Wu et al., 2008) and at an urban background station in Helsinki representing long range transported aerosol (Hussein et al., 2004). The size distribution of the test aerosol used in this study represents well the ambient aerosol measured next to a major road in Helsinki having similar mean particle sizes (NM 10–20 nm, SM 50–70 nm), thus, the TFE for these aerosols are also almost equal. The filtering technologies effective for the smallest particle sizes were observed to produce the highest TFE. Size distribution of the ambient background aerosol in Helsinki is dominated by the accumulation mode and the mean particle size is clearly larger than next to a major road in Helsinki. This affects the TFE of the filters so that the diffusion based filters, such as the F7 and electret filter w/o charger, have the lowest TFE, whereas the electrical separation based filters (electret filter and ESP) remove particles relatively well. In Beijing, the ambient aerosol size distribution has a mean particle size at around 60 nm and the filtration efficiencies calculated for different filters varied between 67.06–99.96%. With the exception of the HEPA filters, the most efficient filter (96.49%) in Beijing would be the electret filter with a charger.

Ultrafine particles (UFP) typically dominate number concentration of ambient aerosols. The major contributors of these aerosols are the combustion aerosols emitted from traffic. The combustion aerosols may contain many carcinogenic compounds such as heavy metals and PAHs (Schauer et a., 1999; Shi et al., 2000). UFP can produce toxic effects even at low concentrations due to their small size and surface characteristics (Johnston et al., 2000). In addition, the non-soluble UFP deposited in the pulmonary region have sufficient time to penetrate into interstitial region and ultimately accumulate there for years (Hussain et al., 2011). The filter technology affects significantly the particle removal efficiency in the UFP size range. To assure healthy indoor air quality level for people, the typical outdoor ambient aerosol concentrations and size distribution as well as filtration technology should be taken into account in building ventilation systems as well as in room air cleaners. Information on the filtration efficiency of commercial

filters in the UFP size range is important, because health risks of these particles are high due to the high lung deposition probability, especially in the alveolar region (ICRP, 1994). Thus, taken into account that particles smaller than 100 nm typically dominate vehicle exhaust particle number emissions and thus typically also the particle number concentration in urban air, it is reasonable to extend the particulate filter test standards in future to cover also the ultrafine particle size range also in other standards than ISO 29463.

## CONCLUSIONS

We have developed a new method for particle generation for particle filtration efficiency tests of ventilation filters. The generation system reproduces a similar exhaust particle size distribution and characteristics as in typical real-world vehicles exhaust aerosol, and a typical size distribution observed next to a major road in Helsinki.

Different types of filters were tested in this study using a new particle generation system consisting of adjustable nucleation and soot particle generators. The nanocluster sized particles below ~3 nm were removed efficiently by the HEPA, F7 and electret filters, the ESP also showed relatively high filtration efficiencies but with increased uncertainty in the determination. For particles larger than 3 nm relatively large variations were observed in the ultrafine particle filtration efficiencies of the tested filter types. The HEPA filters were efficient in all particle sizes. The F7 filter was more efficient for the nucleation particles (below 30 nm), and in contrast, the ESP was more efficient for the soot particles (larger than 30 nm). The electret filter with charger using the advantages of F7 for small particles and the advantages of the ESP for larger particles was efficient in all the particle sizes studied but did not reach the HEPA filtration efficiency levels.

The filters tested in this study were based on very different operational principles. These operational principles practically determined the dominating mechanisms of particle collection

into the filtering media or collection plates, which was seen especially in size dependencies of filtration efficiencies. It can be concluded that for the smallest particles (nanoclusters) the diffusional collection of the particles increased the filtration efficiency, even in the case of the ESP, while for larger particles the use of electrophoresis was an efficient method to increase the filtration efficiency. This was seen especially in studies for the electret filter, which was tested with and without the charger. However, it should be keep in mind that the filtration solutions utilizing electrophoresis may be more efficient for fresh traffic originated soot particles than e.g. for the long-range transported particles in ambient air due to the higher fraction of electrically charged particles in freshly emitted soot.

It should be keep in mind that the filtration efficiency curves were determined in this study under well-controlled laboratory conditions. The changes e.g. in temperature and humidity of air to be purified, filter clogging as well as air flow rate through filter media and maintenance of ventilation systems can affect the filtration efficiencies when these filters are used in real buildings and in real ventilation applications. Thus, the comprehensive understanding of filtration efficiencies require studies in real-world environments too, such as made by Stephens and Siegel (2013).

Based on the results of this study, we suggest that the particulate filter test standards should be extended to cover more comprehensively also the particles smaller than 100 nm in diameter that dominate the vehicle exhaust particle emissions and are potentially hazardous for public health. In future studies, better understanding is needed on the filtration efficiency of ultrafine particles in various types of filtration systems, especially in real environments and with real ambient aerosols.

## ACKNOWLEDGMENTS

Authors acknowledge Matti Niemeläinen for his support in performing the experiments. This work was made in the project “Finnish-Chinese Green ICT R&D&I Living Lab for Energy Efficient, Clean and Safe Environments”, financially supported by Finnish Funding Agency for Innovation (Tekes), and Ahlstrom Oy, FIAC Invest Oy, Green Net Finland Oy, Kauriala Oy, Lassila & Tikanoja Oyj, Lifa Air Oy, MX Electrix Oy, Pegasor Oy and Sandbox Oy.

# REFERENCES


Alderman, S. L., Parsons, M. S., Hogancamp, K. U., & Waggoner, C. A. (2008) Evaluation of the effect of media velocity on filter efficiency and most penetrating particle size of nuclear grade high-efficiency particulate air filters. *Journal of Occupational and Environmental Hygiene*, 5(11), 713-720.

Arnold, F., Pirjola, L., Rönkkö, T. et al. (2012) First online measurements of sulfuric acid gas in modern heavy-duty diesel engine exhaust: Implications for nanoparticle formation. *Environmental Science and Technology*, 46(20), 11227-11234.

ASHRAE (2012) Standard 52.2-2012, *Method of Testing General Ventilation Air-Cleaning Devices for Removal Efficiency by Particle Size (ANSI/ASHRAE Approved)*. American Society of Heating, Refrigerating and Air-Conditioning Engineers.

Chen, L., Ding, S., Liang, Z., Zhou, L., Zhang, H. & Zhang, C. (2017) Filtration efficiency analysis of fibrous filters: Experimental and theoretical study on the sampling of agglomerate particles emitted from a GDI engine, *Aerosol Science and Technology*.

EN 1822-1:2009, *High efficiency air filters (EPA, HEPA and ULPA). Part 1: Classification, performance testing, marking*. European committee for standardization.

EN 1822-2:2009, *High efficiency air filters (EPA, HEPA and ULPA). Part 2: Aerosol production, measuring equipment, particle counting statistics*. European committee for standardization.

Friedlander, S. K. (1958) Theory of aerosol filtration. *Industrial and Engineering Chemistry*, *50*(8), 1161-1164.

375 Giechaskiel, B., Ntziachristos, L., Samaras, Z. et al. (2007) Effect of speed and speed-transition
376 on the formation of nucleation mode particles from a light duty diesel vehicle. *SAE Technical*
377 *Papers*, 2007-01-1110.

378 Goodfellow, H. D., and Tähti, E. (Ed.), (2001). Industrial Ventilation Design Guidebook: 13.
379 Gas-Cleaning Technology. California: Academic Press, 2001, p. 1199.

380 Harris, S.J., Maricq, M.M. (2001) Signature size distributions for diesel and gasoline engine
381 exhaust particulate matter. *Journal of Aerosol Science*, 32 (6), pp. 749-764.

382 Heywood, J. B. (1989) *Internal Combustion Engine Fundamentals*; Mcgraw-Hill: New York, p
383 930.

384 Huang, S. H., and Chen, C. C. (2002) Ultrafine aerosol penetration through electrostatic
385 precipitators. *Environmental Science and Technology*, 36(21), 4625-4632.

386 Hussein, T., Hämeri, K., Heikkinen, M., Kulmala, M. (2005) Indoor and outdoor particle size
387 characterization at a family house in Espoo–Finland, *Atmospheric Environment*, 39, 3697–
388 3709.

389 Hussein, T., Wierzbicka, A., Löndahl, J., Lazaridis, M., Hänninen, O. (2015) Indoor aerosol
390 modeling for assessment of exposure and respiratory tract deposited dose, *Atmospheric*
391 *Environment*, 106, 402 - 411

392 Hussain, M., Winker-Heil, R., & Hofmann, W. (2011). Lung dosimetry for inhaled long-lived
393 radionuclides and radon progeny. Radiation protection dosimetry, ncr060.

394 Hänninen, O., Knol, A. (ed.), Jantunen, M. et al. (2011) European perspectives on Environmental
395 Burden of Disease: Estimates for nine stressors in six countries. *THL Reports 1/2011*,
396 Helsinki, Finland.

397 International Commission on Radiological Protection (ICRP) (1994), Human respiratory tract
398 model for radiological protection. Publication 66. Elsevier Science, Oxford.

399 Jaworek, A., Krupa, A., Czech, T. (2007) Modern electrostatic devices and methods for exhaust
400 gas cleaning: A brief review. *Journal of Electrostatics*, 65(3), 133-155.

401 Johnston, C. J., Finkelstein, J. N., Mercer, P., Corson, N., Gelein, R., & Oberdörster, G. (2000).
402 Pulmonary effects induced by ultrafine PTFE particles. Toxicology and applied
403 pharmacology, 168(3), 208-215.

404 Järvinen, A., Kuuluvainen, H., Niemi, J. V. et al. (2014) Monitoring urban air quality with a
405 diffusion charger based electrical particle sensor. *Urban Climate*.

406 Karjalainen, P., Pirjola, L., Heikkilä, J. et al. (2014a) Exhaust particles of modern gasoline
407 vehicles: A laboratory and an on-road study. *Atmospheric Environment*, 97, 262-270.

408 Karjalainen, P., Rönkkö, T., Pirjola, L. et al. (2014b). Sulfur driven nucleation mode formation in
409 diesel exhaust under transient driving conditions., *Environ. Sci. Technol*., 48(4), 2336–43.

410 Kim, C. S., Bao, L., Okuyama, K. et al. (2006) Filtration efficiency of a fibrous filter for
411 nanoparticles. *Journal of Nanoparticle Research*, 8(2), 215-221.

412 Kim, S. C., Harrington, M. S., Pui, D. Y. (2007) Experimental study of nanoparticles penetration
413 through commercial filter media. *Journal of Nanoparticle Research*, 9(1), 117-125.

414 Kim, S. C., Wang, J., Shin, W. G., Scheckman, J. H., & Pui, D. Y. (2009). Structural properties
415 and filter loading characteristics of soot agglomerates. Aerosol Science and Technology,
416 43(10), 1033-1041.

417 Kittelson, D.B., Watts, W.F., Johnson, J.P. (2004) Nanoparticle emissions on Minnesota
418 highways. *Atmospheric Environment*, 38 (1), pp. 9-19.

419 Kulkarni, P., Baron, P. A., Willeke, K. (Eds.). (2011) *Aerosol measurement: principles,*
420 *techniques, and applications*. John Wiley & Sons.

421 Kuuluvainen, H., Rönkkö, T., Järvinen, A., Saari, S., Karjalainen, P., Lähde, T., Pirjola, L.,
422 Niemi, J.V., Hillamo, R., Keskinen, J. (2016) Lung deposited surface area size distributions
423 of particulate matter in different urban areas. *Atmospheric Environment*, 136, pp. 105-113.

424 Lee, K. W., & Liu, B. Y. H. (1980). On the minimum efficiency and the most penetrating particle
425 size for fibrous filters. Journal of the Air Pollution Control Association, 30(4), 377-381.

426 Li, N., Sioutas, C., Cho, A. et al. (2003) Ultrafine particulate pollutants induce oxidative stress
427 and mitochondrial damage, Environ. Health Perspect., 111, 455–460.

428 Lähde, T., Niemi, J. V., Kousa, A. et al. (2014) Mobile Particle and NOx Emission
429 Characterization at Helsinki Downtown: Comparison of Different Traffic Flow Areas.
430 *Aerosol and Air Quality Research*, 14(5), 1372-1382.

431 Morawska, L., Afshari, A., Bae, G. N. et al. (2013) Indoor aerosols: from personal exposure to
432 risk assessment. *Indoor Air*, 23: 462–487.

433 Oberdörster, G. (2001) Pulmonary effects of inhaled ultrafine particles, Int. Arch. Occup.
434 Environ. Health, 74, 1–8.

435 Pirjola, L., Lähde, T., Niemi, J. et al. (2012) Spatial and temporal characterization of traffic
436 emissions in urban microenvironments with a mobile laboratory. *Atmospheric Environment*,
437 63, 156-167.

438 Pope III, C. A., Thun, M. J., Namboodiri, M. M. et al. (1995) Particulate air pollution as a
439 predictor of mortality in a prospective study of US adults. *American Journal of Respiratory*
440 *and Critical Care Medicine*, 151(3_pt_1), 669-674.

441 Quang, T. N., He, C., Morawska, L., & Knibbs, L. D. (2013). Influence of ventilation and
442 filtration on indoor particle concentrations in urban office buildings. Atmospheric
443 Environment, 79, 41-52.

444 Romay F., J., Liu, B. Y. H. & Chae, S. (1998) Experimental Study of Electrostatic Capture
445 Mechanisms in Commercial Electret Filters, *Aerosol Science and Technology*, 28:3, 224-234.

446 Rostedt, A., Arffman, A., Janka, K. et al. (2014) Characterization and response model of the PPS-
447 M aerosol sensor. *Aerosol Science and Technology*, 48(10), 1022-1030.

448 Rönkkö, T., Virtanen, A., Vaaraslahti, K. et al. (2006) Effect of dilution conditions and driving
449 parameters on nucleation mode particles in diesel exhaust: laboratory and on-road study.
450 *Atmospheric Environment*, 40, 2893-2901.

451 Rönkkö, T., Virtanen, A., Kannosto, J. et al. (2007) Nucleation mode particles with a nonvolatile
452 core in the exhaust of a heavy duty diesel vehicle. *Environmental Science and Technology*,
453 41, 6384-6389.

454 Rönkkö, T., Pirjola, L., Ntziachristos, L. et al. (2014) Vehicle engines produce exhaust
455 nanoparticles even when not fueled. *Environmental Science and Technology*, 48, 2043–2050.

456 Saarikoski, S., Timonen, H., Saarnio, K. et al. (2008) Sources of organic carbon in fine
457 particulate matter in northern European urban air. *Atmospheric Chemistry and Physics*, 8(20),
458 6281-6295.

459 Schauer, J. J., Kleeman, M. J., Cass, G. R. and Simoneit, B. R. T. (1999) Measurement of
460 emissions from air pollution sources. 2. C1 through C30 organic compounds from medium
461 duty diesel trucks, *Environ. Sci. Technol.*, 33(10), 1578–1587. doi:10.1021/es980081n, 1999.

462 Shi, B. (2012) Removal of ultrafine particles by intermediate air filters in ventilation systems.
463 Evaluation of performance and analysis of applications. PhD Thesis, Chalmers University of
464 Technology.

465 Shi, B., Ekberg, L. E., Langer, S. (2013). Intermediate air filters for general ventilation
466 applications: An experimental evaluation of various filtration efficiency expressions. *Aerosol*
467 *Science and Technology*, 47(5), 488-498.

468 Shi, J., Mark, D., Harrison, R. (2000) Characterization of Particles from a Current Technology
469 Heavy-Duty Diesel Engine, *Environmental Science & Technology*, 34, 748-755.

470 Stephens, B., Siegel, J.A. (2013) Ultrafine particle removal by residential heating, ventilating,
471 and air-conditioning filters, *Indoor Air*, 23 (6), pp. 488-497.

472 David Sinclair (1976), Penetration of hepa filters by submicron aerosols, *Journal of Aerosol*
473 *Science*, Volume 7, Issue 2, Pages 175-179.

474 Tobias, H. J., Beving, D. E., Ziemann, P. J. et al. (2001) Chemical analysis of diesel engine
475 nanoparticles using a nano-DMA/thermal desorption particle beam mass spectrometer.
476 *Environmental Science and Technology*, 35, 2233–2243.

477 Valmari, T., Lehtimäki, M., Taipale, A. (2006) Filter clogging by bimodal aerosol, *Aerosol*
478 *Science and Technology*, 40 (4), pp. 255-260.

479 Virtanen, A., Rönkkö, T., Kannosto, J. et al. (2006) Physical characteristics of winter and
480 summer time emissions of busy road at Helsinki. *Atmospheric Chemistry and Physics*
481 *Discussion*, 6, 549-578.

482 WHO (2012) Report: Diesel engine exhaust carcinogenic, International Agency for Research on
483 Cancer, World Health Organization

484 Wichmann, H.E. and Peters, A. (2000) Epidemiological evidence of the effects of ultrafine
485 particle exposure, Philos. Trans. R. Soc. Lond. A, 358, 2751–2768.

486 Wu, Z., Hu, M., Lin, P., Liu, S., Wehner, B., Wiedensohler, A. (2008) Particle number size
487 distribution in the urban atmosphere of Beijing, China, *Atmospheric Environment* 42,7967–
488 7980.

489

490 **Table 1.** Description of the tested filters: F7, HEPA 1, HEPA 2, Electret, ESP. Errors for
491 pressure drop, volumetric flow and face velocities have been determined by the information
492 provided by the device manufacturers.

| | F7 | HEPA 1 | HEPA 2 | Electret | ESP |
|---|---|---|---|---|---|
| | 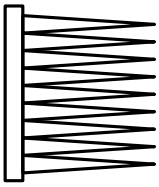 | 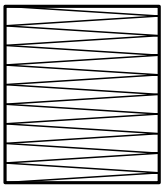 | 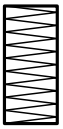 | 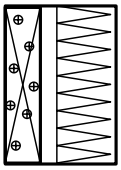 | 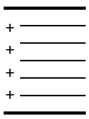 |
| Dimensions (mm) | 610×610×620 | 610×610×580 | 295×295×120 | 610×610×600 | 525×325×205 |
| Pressure drop (Pa) | 43±0.5 | 152±0.5 | 90±0.5 | 115±0.5 | 3±0.5 |
| Volumetric flow (l/s) | 500±25 | 500±25 | 53±2.6 | 500±25 | 170±8.5 |
| Face velocity (m/s) | 1.34±0.07 | 1.34±0.07 | 0.61±0.03 | 1.34±0.07 | 1±0.05 |

493

494

## Figure Captions

**Fig. 1.** Experimental setup consisting of aerosol particle generators (both nucleation and soot), mixing chamber, ventilation channel, test filters, dilution and aerosol measurement instruments.

**Fig. 2.** Example of the upstream particle size distribution used in the experiments (blue line) and the fraction of electrically charged particles (oranged line). Zoomed size distribution shows the particle concentrations in the PSM detection size range.

**Fig. 3.** Stability of the aerosol generation system measured by the Nano-SMPS (blue, $D_p < 20$ nm) and Long-SMPS (green, $D_p > 20$ nm) (top), and by the ELPI (total particle concentration, $D_a > 30$ nm) (bottom).

**Fig. 4.** Particle filtration efficiencies for the tested filters calculated from upstream and downstream size distributions measured by the PSM ($D_p$ 1.3-2.9 nm), Nano-SMPS ($D_p$ 3 - 20 nm) and Long-SMPS ($D_p > 20$ nm).

**Fig. 5.** Uppermost row shows the normalized particle size distributions from the left: NM (this study), SM (this study), test aerosol (this study), Helsinki road side (Virtanen et al., 2006), Peking (Wu et al. (2008)), Helsinki accumulation mode (AM) only (Hussein et al. (2004)). The rows below indicate what size distribution exists indoor after row corresponding filtration, and the percentages indicate the total number filtration efficiency for the corresponding aerosol.

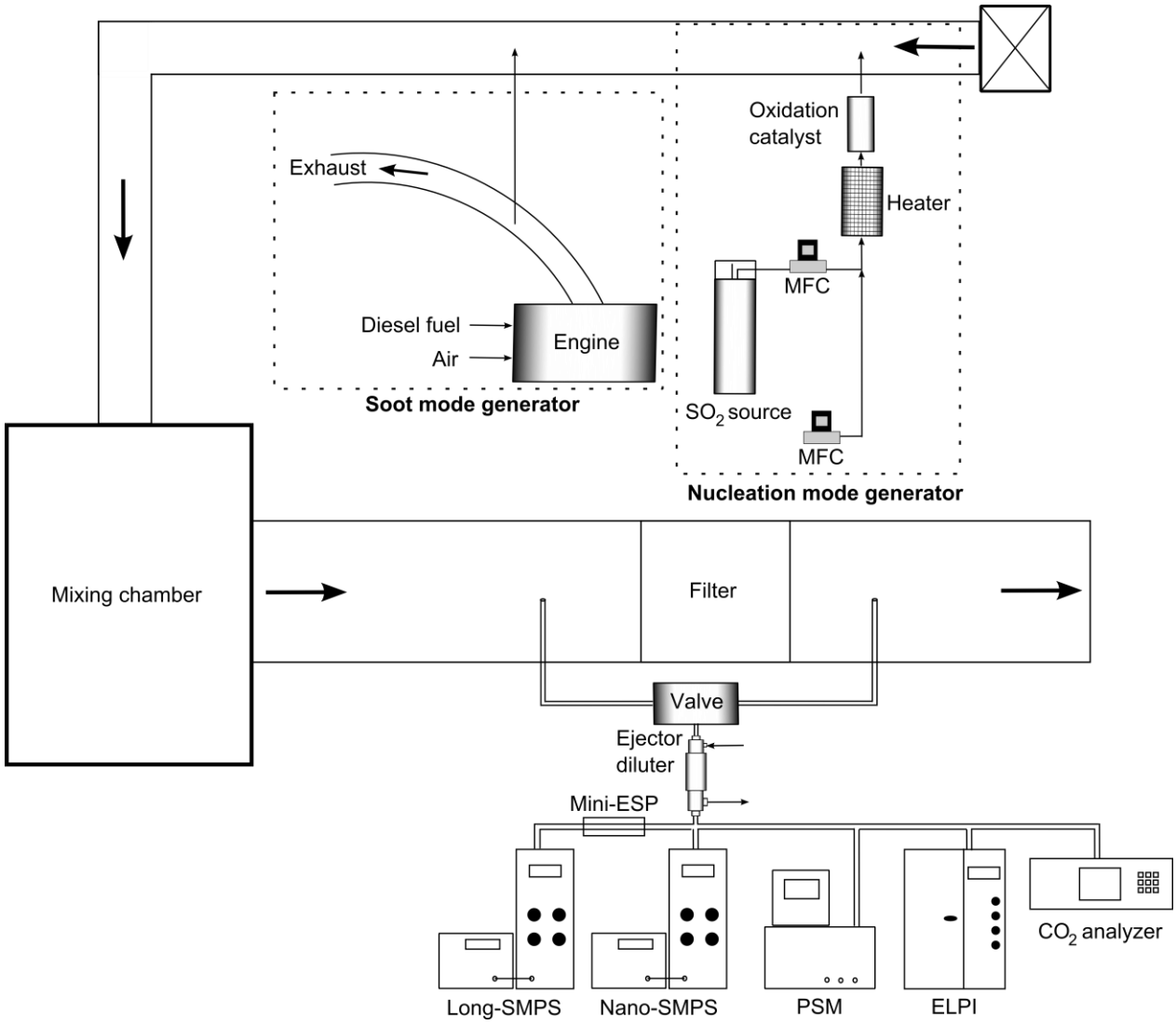


514

515 **Fig. 1.**

516

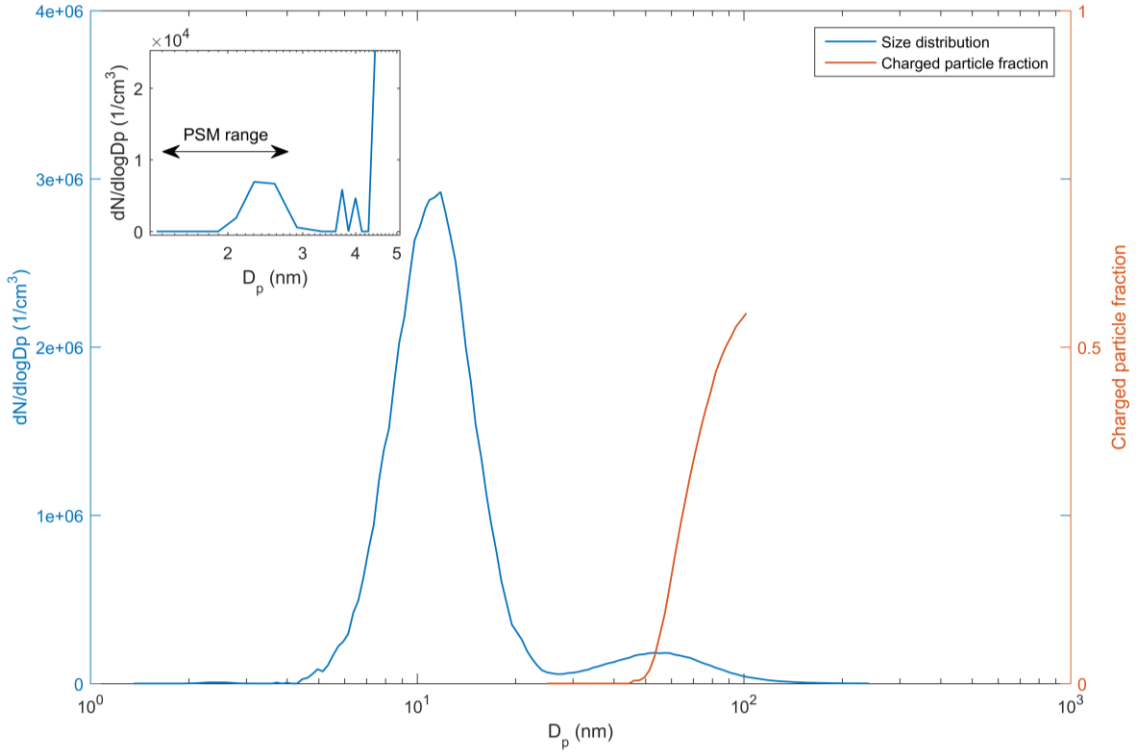


517

518 **Fig. 2.**

519

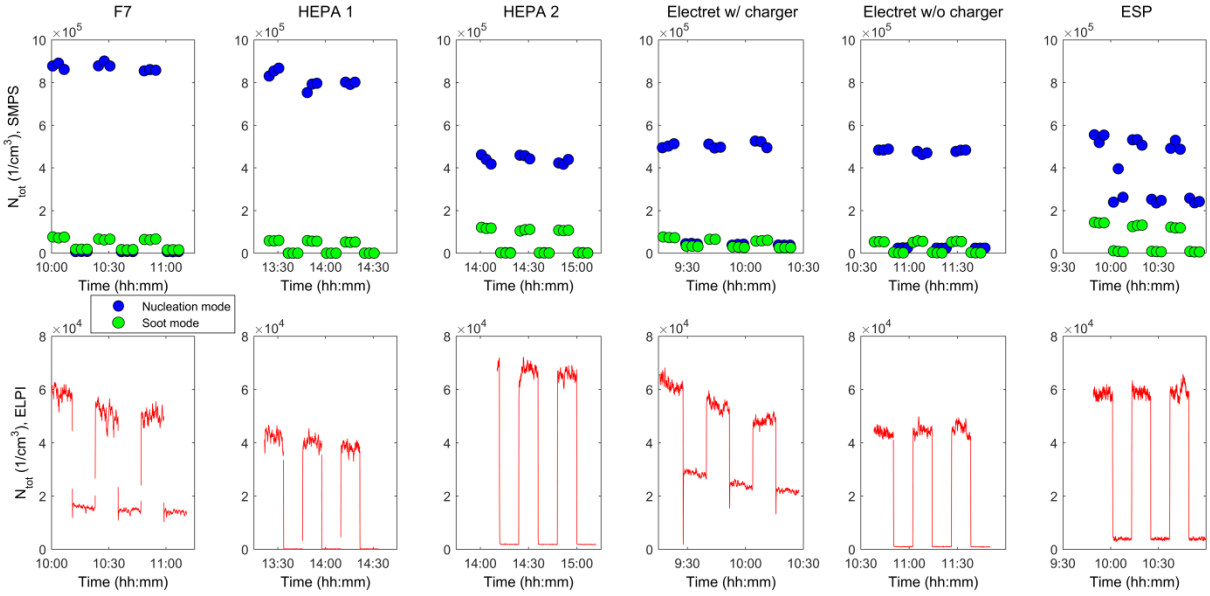


520

521 **Fig. 3.**

522

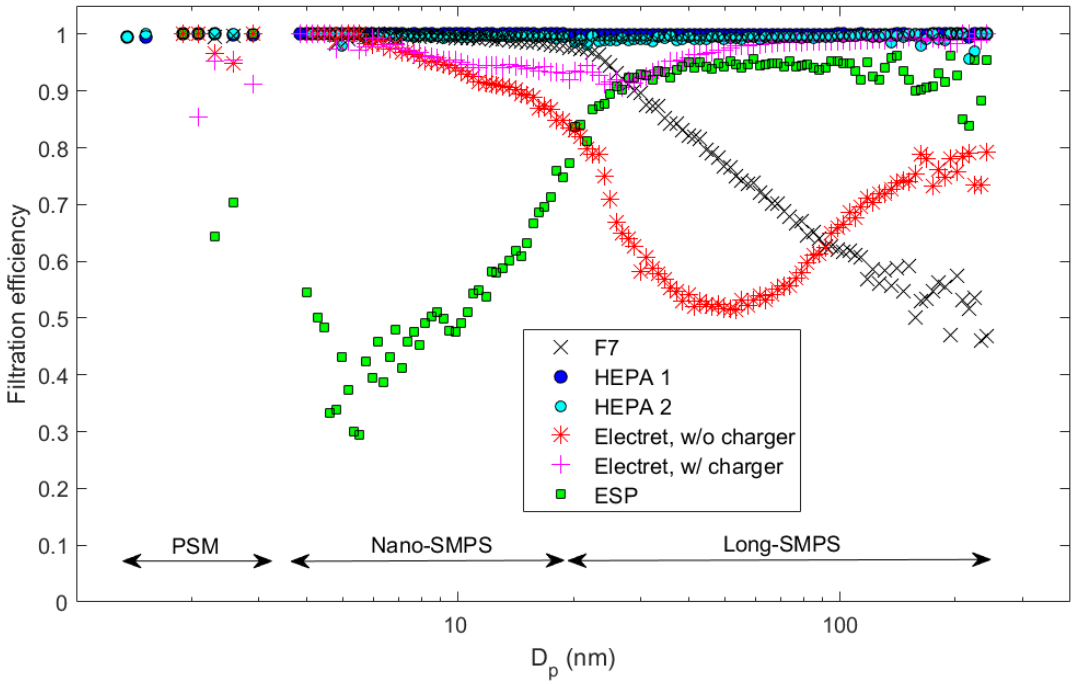


523

524 **Fig. 4.**

525

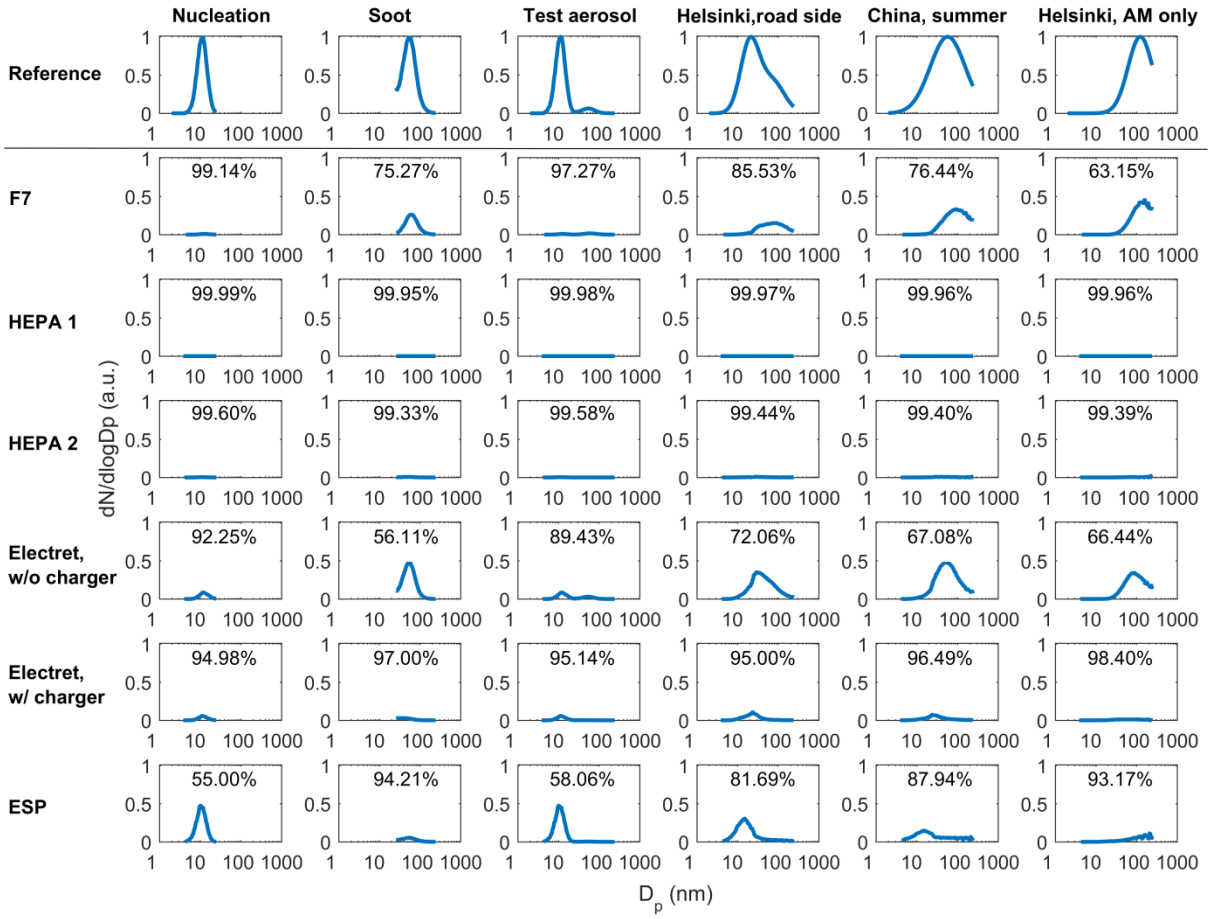
Nucleation
Soot
Test aerosol
Helsinki,road side
China, summer
Helsinki, AM only
Reference
F7
HEPA 1
HEPA 2
Electret, w/o charger
Electret, w/ charger
ESP
99.14%
75.27%
97.27%
85.53%
76.44%
63.15%
99.99%
99.95%
99.98%
99.97%
99.96%
99.96%
99.60%
99.33%
99.58%
99.44%
99.40%
99.39%
92.25%
56.11%
89.43%
72.06%
67.08%
66.44%
94.98%
97.00%
95.14%
95.00%
96.49%
98.40%
55.00%
94.21%
58.06%
81.69%
87.94%
93.17%
dN/dlogDp (a.u.)
D_p (nm)

526

527 **Fig. 5.**